An Improved Signal Model for Axion Dark Matter Searches

Erik W. Lentz[1]

[1] Physics Department, University of Washington, Seattle, WA 98195-1580

DOI: http://dx.doi.org/10.3204/DESY-PROC-2017-02/lentz_erik

To date, most direct detection searches for axion dark matter, such as those by the Axion Dark Matter Experiment (ADMX) microwave cavity search, have assumed a signal shape based on an isothermal spherical model of the Milky Way halo. Such a model is not capable of capturing contributions from realistic infall, nor from a baryonic disk. Modern N-Body simulations of structure formation can produce realistic Milky Way-like halos which include the influences of baryons, infall, and environmental influences. An analysis of the Romulus25 N-Body simulation shows that the axion signals from MW-like halos are narrower than the SHM by nearly a factor of two, which has important implications for cavity searches. An improved signal shape and an account of the relevant halo dynamics are also given. This proceedings largely follows the recent publication by Lentz et al.[14] (L2017).

1 Introduction

The QCD axion is a compelling candidate for the dark matter (DM), with well-bounded parameter space of mass and coupling, Fig.1. Starting at milli-eV masses, there is a bound above which the axion would have been seen in various astrophysical processes [19, 9, 6, 27, 16, 15]. Approaching micro-eV masses, there is a bound below which the (misalignment) creation mechanism would produce more axions than there is dark matter [1, 8, 18, 16]. This lower bound is somewhat soft as axion creation mechanisms can be suppressed in the details of some axion theories [15]. The two diagonal lines represent benchmark axion models. KSVZ represents a theory where the axion couples to hadrons only [12, 22], and DFSZ couples to both hadrons and leptons [7, 28] as consistent with grand unified theories. The search window is then given by the region between KSVZ and DFSZ and the lower and upper mass bounds.

The axion's low mass and feeble couplings lead to unconventional search techniques. An attractive method used to search for axion DM threads a magnetic field through a resonant cavity, stimulating the decay of DM axions into microwaves via an inverse Primakov process parameterized by the Lagrangian

$$\mathcal{L}_{int} = \frac{g_{a\gamma\gamma}}{4\pi} a F \tilde{F} \tag{1}$$

where a is the axion field, F and $\tilde{F}$ are the electromagnetic field strength and its dual, and $g_{a\gamma\gamma}$ is the coupling strength [23]. Nearly all the power from axion decays is transfered into microwaves of frequency set by the decayed axion energy

$$E_\gamma = \hbar\nu = m_a c^2 + m_a v^2/2 \tag{2}$$

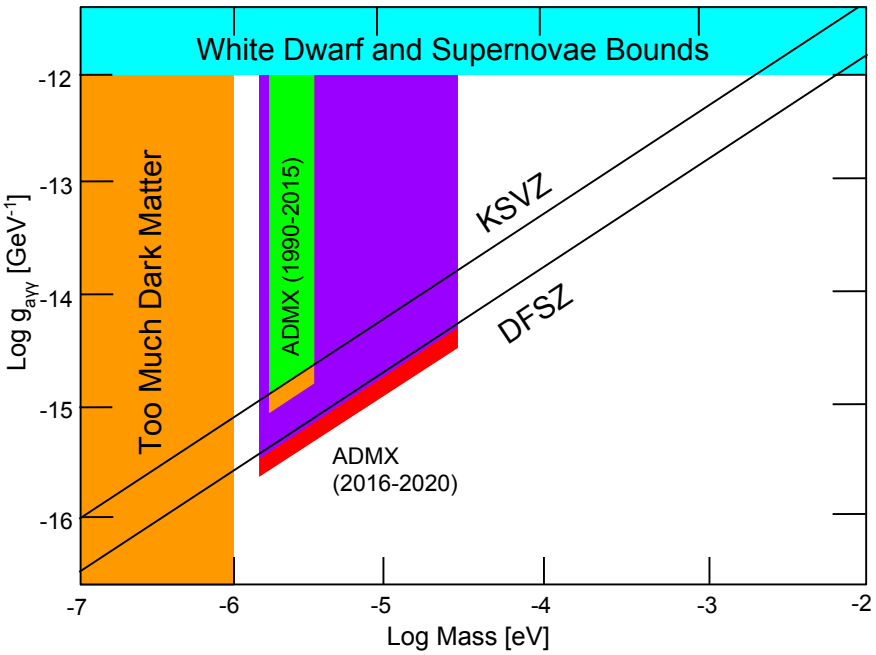

Figure 1: Illustration of the QCD axion parameter space over the plausible DM region, with current astronomical and cosmological constraints, benchmark theories, plus the ADMX limits in green and Generation 2 projections shown in purple Under the new signal model, an increase of the SNR of 1.8 would translate to an improvement in the coupling limit of $\sqrt{1.8}$, illustrated in orange and red respectively.

where m_a is the axion mass, v is the axion speed in the lab frame, and ν is the microwave frequency. The energy distribution of axions is sampled by tuning the cavity over large ranges in frequency, making the microwave power spectrum the figure of interest. The resonant microwaves are detected by a receiver sensitive to sub-yocto-watt power. These experiments can have frequency resolution to a part in 10^9 or better [2], well within the range of resolving fine structure in the axion distribution.

Some axion searches use a filter shape derived from the Standard Halo Model (SHM) despite their good energy resolution [2], which comes from the assumption that the MW halo is given by a thermalized pressure-less self-gravitating sphere of particles. The velocity distribution of the SHM near the Earth is given by a Maxwellian distribution below the escape velocity

$$f_{\vec{v}} \propto e^{-\vec{v}\cdot\vec{v}/2\sigma_v^2} \tag{3}$$

where $\sigma_v = v_c/\sqrt{2}$ [3] and the v_c is the circular speed. The SHM is broadly predictive, but incapable of describing fine structure due to cosmological infall history, interactions with baryonic matter, or axion-specific physics.

Infall history and baryonic interactions in galaxies like the MW can instead be simulated using modern structure-formation techniques. One powerful simulation tool is the N-Body+Smoothed-Particle Hydrodynamics (N-Body+SPH) method. Capable of accurately re-

solving the inner structures of galaxies and their halos using cold dark matter and well-calibrated baryonic models, N-Body+SPH simulations are poised to give accurate models of DM structure for direct searches. This has already been done for WIMPs, which have not yielded significant differences from the SHM [24, 11, 5]. As the energy spectra for cavity axion searches is different from the speed spectra relevant to WIMP nuclear recoil searches, an axion-specific analysis of structure-formation simulations is worthwhile.

2 Approach and Results

This study utilizes the results of the Romulus 25 (R25) N-Body+SPH simulation produced by the UW N-Body Shop [26], based on the ChaNGa N-Body+SPH code. R25 was created on the Blue Waters petascale computing facility. To analyze specific galaxies and halos in R25, the Amiga Halo Finder (AHF) [13] is used to create the catalogue on R25, also at Blue Waters. Finally, the analysis was greatly assisted by the Pynbody N-body analysis software package [17].

R25 describes a 25 Mpc periodic cosmological box filled with DM particles, evolving gas and star particles, and super-massive black holes (SMBHs). The box is placed in a ΛCDM cosmological setting and resolved to $10^5 M_\odot$ particle resolution and 250 pc plummer-equivalent force resolution; these are more than sufficient to resolve the local axion distribution on the kpc scale. R25 is large enough that it has O(30) MW-mass halos at z=0. Such a large set allows for a sampling of galaxies where reduction down to a MW-like sample is quantifiable via the use of filters on a halos catalogue.

The galaxy halos analyzed here are selected using filters in line with the current understanding of MW halo mass, rotational velocity structure, and relatively quiet recent formation history [4, 10, 21] without being so constraining as to limit halo statistics.

$$0.5 \times 10^{12} M_\odot \leq M_{vir} \leq 1.6 \times 10^{12} M_\odot \tag{4}$$

$$R_{vir} \leq 250 \text{ kpc} \tag{5}$$

$$z_{major} \geq 0.75 \tag{6}$$

$$175 \text{ km/s} \leq v_{circ} \leq 275 \text{ km/s} \tag{7}$$

where M_{vir} is the virialized mass, R_{vir} is the enclosing virial radius, and z_{major} is the redshift of last major merger, which is set by the progenitor ratio of 4:1. Several halos experienced no major mergers during the simulation. v_{circ} is the circular velocity in the plane of the galaxy at 8 kpc, which did eliminate several halos from the set satisfying Eqs.4 -6. R25 contains 16 halos which satisfy the filters at $z = 0$, which still cover a wide morphological range.

Terrestrial DM search experiments are moving with respect to the galactic center. The lab is held to be in the galaxy's local standard of rest, approximated as a circular orbit about the center of the galaxy of $r_l = 8$ kpc, coincident with the Sun-MW orbital shape and radius. The solar sample of particles is given by a 2 kpc by 4 kpc toroid about the solar orbit, which is taken to be in the baryonic disk,

$$-2 \text{ kpc} \leq z \leq 2 \text{ kpc} \ , \ r_l - 1 \text{ kpc} \leq r \leq r_l + 1 \text{ kpc} \tag{8}$$

where r_l is chosen to match the MW solar radius of 8 kpc, though the spectral shapes are reasonably robust to the choice of radius. Halo sample energy spectra are formed by calculating the energy for each particle and compiling a normalized histogram over all sample particles.

The orbit speed of the lab is given by setting the acceleration of disk particles at the orbit radius to orbital motion

$$\bar{a}(r_l) = \frac{v_l^2}{r_l} \tag{9}$$

where the RHS is the centripetal acceleration of the lab frame and $\bar{a}$ is the average acceleration at the lab radius. In order to approximate the velocity distribution in a point-like lab, this sample region assumes a cylindrically symmetric, homogeneous, equi-potential, steady-state system within. To evaluate the particles in the lab frame, a Galilean boost is performed on each sample particle using the solar orbital velocity

$$(v_r, v_t, v_z) \rightarrow (v_r, v_t - v_l, v_z) \tag{10}$$

where v_l is taken to be the circular velocity in the presence of DM+baryons at the orbit radius and v_r, v_t, v_z are a particle's radial, tangential, and z-component velocities respectively. The laboratory speed, energy, and other spectra can now be calculated by forming distribution functions over the desired observable.

The lab frame microwave spectra show a marked difference from the SHM, Fig.2. This apparent narrowing and enhancement of the signal is present over all but one of the 16 halos. Also, recall that filters in Eqs.4 -7 allow galaxies which deviate from the MW. Specifically, the galaxies inside halos h32, h34, h36, h44, and h48 have older stars and larger bulges than is expected for the MW. These galaxies lower the mean deviation as they produce spectra preferentially closer to the SHM than the rest of the halos; such halos are still included, as filters based on morphology are not considered here.

The characteristic spectral shape over a wide range of galaxies communicates a level of robustness in the line shape and gives confidence in a signal model based on these spectra. The solid black line of Fig.2 represents the fitted model signal shape. The proposed signal shape keeps a Maxwellian-like form

$$f_\nu \propto \left(\frac{(\nu - \nu_o)h}{m_a T}\right)^\alpha e^{-\left(\frac{(\nu-\nu_o)h}{m_a T}\right)^\beta} \tag{11}$$

where the parameters are constrained to be positive. The best-fit parameters are found using a log-normal local M-estimate using parameter data from individually least-squares-fit halos and are calculated to be $\alpha = 0.36 \pm 0.13$, $\beta = 1.39 \pm 0.28$, and $T = (4.7 \pm 1.9) \times 10^{-7}$, with the errors given by the roots of covariance matrix diagonals.

The narrowing of the observed shapes has implications for axion search experiments. The modeled signal shape has a 90% width—the minimum span which contains 90% of the distribution—that is 1.8 times narrower than the SHM. Such a narrowing of the signal shape would improve a search's SNR by the same factor. For an axion cavity search like ADMX, the increase in sensitivity translates to an improvement in the coupling limit of $\sqrt{1.8}$, suggesting past data runs [2, 25] have near-DFSZ sensitivity, Fig.1.

Observations of local velocity distributions show two main causes of the narrow spectra: bulk rotation and velocity anisotropy. These halo features are very similar to what is expected in a dark disk, where the baryonic disk pulls DM into co-rotating orbits. A DM-only version of R25 (R25D), created before the full SPH run, produces many of the same halos as the full run including our MWs. Analogue halos are pulled to provide insight as to how the baryons contribute to the signal narrowing.

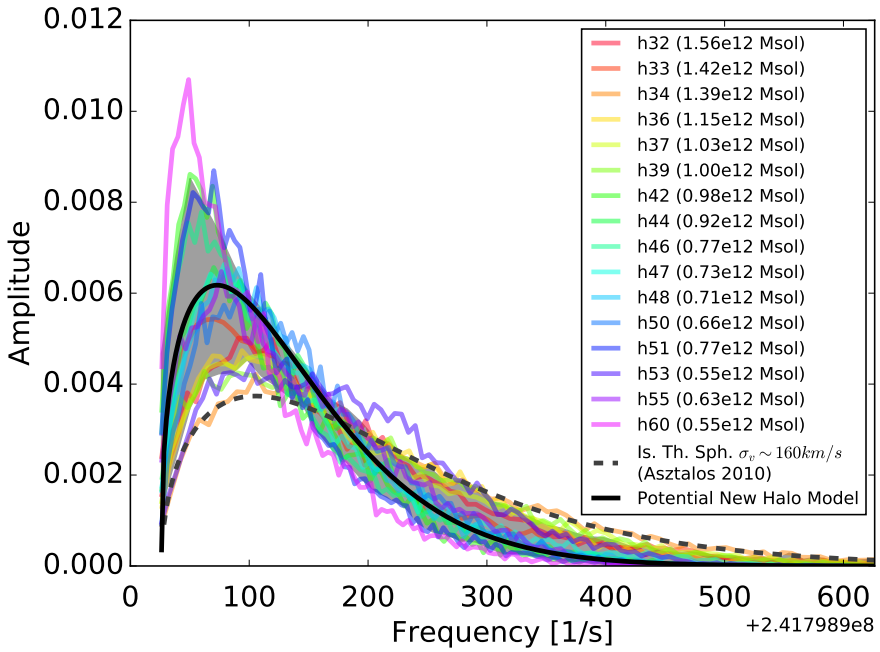

Figure 2: Frequency spectra of MW-like halos from Romulus25 at $z = 0$ and the SHM composed of 10^{-6} eV c^{-2} axions, given by Figure 3 of L2017. The solid black line represents the new shape of the form Eq.11 fitted to to the halos, with the gray representing the data-based error estimate using the two-thirds rule.

The local axion spectra for the R25D halos are not wider but narrower! Fig.3. Bulk motions appear to remain stationary in the median but with decreased dispersion, in contradiction with the existence of a dark disk. Another important kinematical difference becomes apparent when comparing the two halo types: temperature. The effective speed dispersion increases significantly when baryons are included. An increase in circular velocity is also observed. Both the heating and velocity increase are caused by an amplification of the total core mass due to the presence of the galaxy. The sum of these impacts are sufficient to account for the widening factors observed. Baryons don't cause a narrower signal, the signal appears to be narrower in spite of the baryons!

3 Summary

Halos from the Romulus25 simulation show major differences from the SHM in spectra relevant to axion DM searches. The class of galaxies satisfying the above constraints, which include the MW, are observed to produce significantly narrower DM energy spectra than the SHM. A conservative estimate of the new shape is constructed and serves to improve the signal-to-noise of axion cavity searches by 1.8, increasing the sensitivity of previous analyses and improving

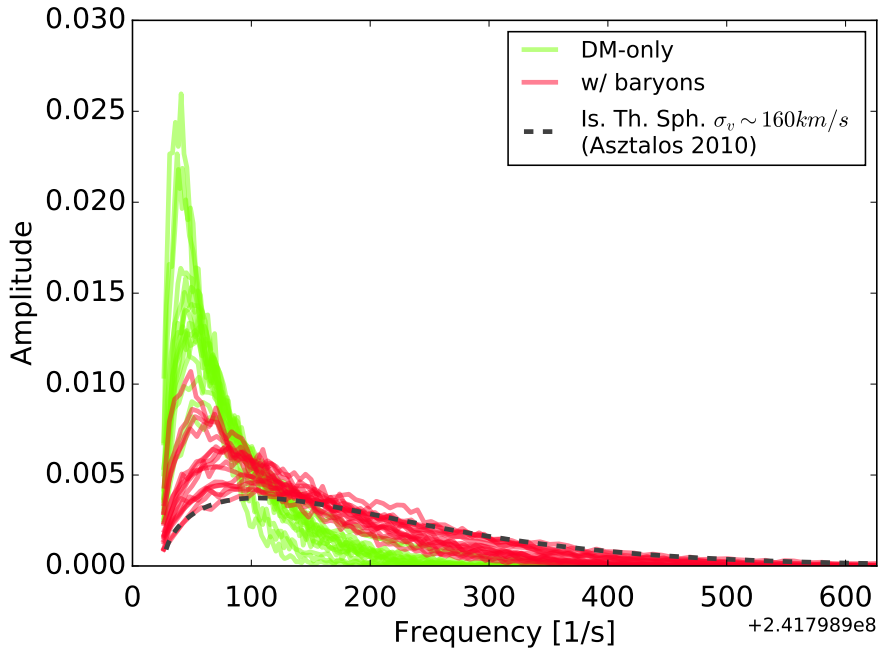

Figure 3: Frequency spectra of MW-like halos from Romulus25 at $z = 0$ and the SHM composed of 10^{-6} eV c^{-2} axions. The solid black line represents the new shape fitted to to the halos, with the gray representing the data-based error estimate using the two-thirds rule.

future observations through the option of scanning at a higher sensitivity or a higher search rate. The kinematical causes for narrowing appears to be bulk rotational motions, velocity anisotropy, and heating. Baryon potentials do not cause this narrowing but serve more to disrupt it. Preliminary studies of the dynamics point to the resonant nature of collision-less gravitational virialization. Research is underway to further classify these dynamical causes.

4 Acknowledgements

I gratefully acknowledge the support of the U.S. Department of Energy office of High Energy Physics, supported by the DOE grant DE-SC0011665. This research is part of the Blue Waters sustained-petascale computing project, which is supported by the National Science Foundation (awards OCI-0725070 and ACI-1238993) and the state of Illinois. Blue Waters is a joint effort of the University of Illinois at Urbana-Champaign and its National Center for Supercomputing Applications. This work is also part of a PRAC allocation support by the National Science Foundation (award number OCI-1144357).

References

[1] Abbott, L. F., Sikivie, P., 1983, PhLB 120, 133

[2] Asztalos, S., Carosi, G., Hagmann, C., et al., 2010, PhRvL, 104d1301A

[3] Binney, J., Tremaine, S., 2008, Princeton Univ. Press, ISBN-13: 978-0-691-13026-2

[4] Bovy, J., Allende Prieto, C., Beers, T., et al., 2012, ApJ, 759, 131

[5] Bozorgnia, N., Calore, F., Schaller, M., et al., 2016, JCAP, 05, 024B

[6] Corsico, A., Althaus, L., L., Romero, A., et al., 2012, JCAP 1212, 010

[7] Dine, M., Fischler, W., Srednicki, M., 1981, PhLB, 104, 199D

[8] Dine, M., Fischler, W., 1983, PhLB 120, 137

[9] Isern, J., Garcia-Berro, E., Althaus, L., et al., 2010, A&A, 512A, 86I

[10] Kafle, P., Sharma, S., Lewis, G., Bland-Hawthorn, J., 2012, ApJ, 761, 98

[11] Kelso, C., Savage, C., Valluri, M., et al., 2016, JCAP, 08, 071K

[12] Kim, J., 1979, PhRvL, 43, 103K

[13] Knollmann, S., Knebe, A., 2009, ApJS, 182, 608K

[14] Lentz, E., Quinn, T., Rosenberg, L., Tremmel, M., 2017, ApJ, 845, 121L

[15] Marsh, D., 2016, PhR, 643, 1M

[16] C. Patrignani et al. (Particle Data Group), 2016, Chin. Phys. C, 40, 100001

[17] Pontzen, A., Roškar, R., Stinson, G., Woods, R., 2013, pynbody:N-Body/SPH analysis for python, Astrophysics Source Code Library

[18] Preskill, J., Wise, M. B., Wilczek, F., 1983, PhLB 120, 127

[19] Raffelt, G. G., 2008, LNP, 741, 51R

[20] Reid, M. J., Menten, K. M., Brunthaler, A., et al., 2014, ApJ, 783, 130R

[21] Ruchti, G., Read, J., Feltzing, S., et al., 2015, MNRAS, 450, 2874

[22] Shifman, M., Vainshtein, A., Zakharov, V., 1980, NuPhB, 166, 493S

[23] Sikivie, P., 1983, PhRvL, 51, 1415

[24] Sloane, J., Buckley, M., Brooks, A., et al., 2016, ApJ, 831, 93S

[25] Stern, I., ADMX, ADMX-HF Collaborations, 2014, AIPC, 1604, 456S

[26] Tremmel, M., Karcher, M., Governato, F., et al., 2017, MNRAS, 470, 1121T

[27] Viaux, N., Catelan, M., Stetson, P. B., et al., 2013, A&A, 558, 12V

[28] Zhitnitsky, A., 1980, Sov. J. Nucl. Phys., 31, 260